Int. J. Heat Mass Transfer. Vol. 33, No. 5, pp. 917–930, 1990
Printed in Great Britain

0017–9310/90 $3.00 + 0.00

Natural convection in a two-dimensional square loop

EDUARDO RAMOS and ALFREDO CASTREJÓN
Laboratorio de Energía Solar IIM-UNAM, 62580 Temixco Mor., Mexico

and

MANUEL GORDON
Universidad Autónoma Metropolitana, 02000 México, D.F. Mexico

(*Received* 27 *April* 1988 *and in final form* 25 *August* 1989)

Abstract—The present investigation deals with the steady-state natural convective flow inside a two-dimensional square loop. Opposite legs of the loop are held at constant but different temperatures and therefore, due to the presence of gravity, fluid motion ensues; viscous effects resist the motion and a steady-state flow is reached. The geometry of the loop is fixed but several temperature differences have been considered. Also, the effect of the tilt angle on the flow patterns has been analyzed. Local recirculating motions are the dominant features of the flow when the upper walls are at higher temperature than the lower ones. In contrast, a single global cell appears when the loop is tilted. Double solutions have been found for tilt angles close to zero (high temperature at the bottom walls); the size of the tilt angle interval where double solutions exist has been determined as a function of the Rayleigh number. One-dimensional models have predicted multiple steady-state solutions in systems similar to the one studied here; in the present paper, the existence of multiple solutions in a two-dimensional model has been demonstrated.

1. INTRODUCTION

NATURAL CONVECTIVE loops have been the subject of study of numerous investigations both from the basic and applied science viewpoints. A review which emphasizes the heat transfer properties of these systems and describes their various applications has been published by Mertol and Greif [1]. Although the picture of the qualitative behavior of the flow in such systems has been slowly emerging, the full description is far from being available at present. One of the pioneering studies on the subject that unraveled the complexity of the phenomenon is the work of Creveling *et al.* [2], who used a thin toroidal loop of tubing filled with water to observe its dynamic behavior. The lower half of the loop was electrically heated and the wall temperature of the upper half was maintained at a constant value. They observed flows with constant velocity circulating clockwise or counter-clockwise for the same external conditions; using higher heating rates, they found flows featuring aperiodic oscillations.

One-dimensional theoretical models presently available (see for instance ref. [3], [4] or [5]), identify the constant velocity flows with stable critical points in the phase space of a dynamic system describing the flow. Oscillations appear when the critical points become unstable. Most theoretical models are one-dimensional and some physical effects are incorporated through empirical expressions. In particular, viscous effects are taken into account by assuming the existence of a sink linearly proportional to the velocity in the momentum balance equation. These theoretical interpretations have succeeded in describing some of the qualitative features of the phenomenon, but it is not clear to what extent the results depend on the particular choice of the empirical information incorporated which is, in some instances, a crude model of reality. Also, no quantitative information can be obtained from the one-dimensional models for experimental verification due to the empirical information involved. By definition, no two- or three-dimensional effects can be studied and consequently some characteristics of the flow are not modeled. This omission is not expected to be very important when the characteristic length of the loop is large compared with the cross-section of the tubing forming the loop. However, in 'fat' loops, two- or three-dimensional effects can be of prime importance. Two-dimensional numerical models have been used to study the flow in a toroidal thermosyphon [6, 7]; no empirical information was required in order to account for the viscous resistance or the heat transfer at the walls, as the friction factor and the Nusselt number were obtained as part of the solution. The theoretical mass flow rate obtained as a function of the heat input with the two-dimensional model was compared favorably in the laminar steady-state regime with the experimental results of ref. [2]. A three-dimensional numerical model for a toroidal loop was proposed in ref. [8]; flow reversals and secondary flows were reported. These features were observed experimentally by Damerell and Schoenhals [9] but no formal comparison of theoretical and experimental results is available as yet. Moreover, some general characteristics of the flow still remain to be clarified. For

NOMENCLATURE

d	dimensional duct width
g	gravitational acceleration
H	length of the outer wall of the loop
Nu	Nusselt number
p	dimensionless pressure, $\rho\nu^2 p'/H^2$
Pr	Prandtl number, ν/α
Ra	Rayleigh number, $g\beta\Delta T d^3/\nu\alpha$
T	dimensionless temperature, $(T'-T'_C)/(T'_H-T'_C)$
u	dimensionless velocity in the x-direction, $u'H/\nu$
v	dimensionless velocity in the y-direction, $v'H/\nu$
x	dimensionless spatial coordinate, x'/H
y	dimensionless spatial coordinate, y'/H.

Greek symbols

α	thermal diffusivity
β	thermal expansion coefficient
γ	tilt angle
δ	non-dimensional duct width, d/H
ν	kinematic viscosity
Ψ	dimensionless stream function, Ψ'/ν.

Subscripts

0	reference value
C	cold temperature
H	hot temperature
M	maximum value
m	minimum value.

Superscript

	dimensional variables.

instance, it is well known from one-dimensional models that the system displays multiple solutions [10, 11]. Also, aperiodic oscillations in loops have been analyzed with one-dimensional models in the context of dynamical systems theory and their structures in the phase-space have been associated with strange attractors. A general multi-dimensional theory addressing these points where no empirical information is involved has not been presented to date.

In this paper we analyze the steady-state flow in a square two-dimensional thermosyphon with particular emphasis on the existence of multiple solutions in order to generalize the steady-state, one-dimensional theory.

2. MATHEMATICAL MODEL

Consider a two-dimensional square duct filled with a fluid, and tilted at an angle γ with respect to the horizontal as shown in Fig. 1. The wall temperatures of two opposite legs are held at constant but different temperatures T'_C and T'_H while the other two legs are thermally insulated. The length of the external wall of the legs is denoted by H and the duct width by d. The fluid moves inside the loop due to the buoyancy force generated by the density gradients. The working fluid is Newtonian and incompressible; viscous dissipation is neglected in the energy equation and it is assumed that the Boussinesq approximation is applicable.

Under steady-state conditions and referred to the tilted axes, the governing equations written in terms of the non-dimensional variables defined in the nomenclature are:

mass balance

$$\frac{\partial u}{\partial x}+\frac{\partial v}{\partial y}=0;$$

momentum balance

x-direction

$$u\frac{\partial u}{\partial x}+v\frac{\partial u}{\partial y}=-\frac{\partial p}{\partial x}+\frac{\partial^2 u}{\partial x^2}+\frac{\partial^2 u}{\partial y^2}-\frac{Ra}{\delta^3 Pr}T\sin\gamma$$

y-direction

$$u\frac{\partial v}{\partial x}+v\frac{\partial v}{\partial y}=-\frac{\partial p}{\partial y}+\frac{\partial^2 v}{\partial x^2}+\frac{\partial^2 v}{\partial y^2}-\frac{Ra}{\delta^3 Pr}T\cos\gamma;$$

energy balance

$$u\frac{\partial T}{\partial x}+v\frac{\partial T}{\partial y}=\frac{1}{Pr}\left\{\frac{\partial^2 T}{\partial x^2}+\frac{\partial^2 T}{\partial y^2}\right\}$$

where u and v are the velocities in the x- and y-directions respectively, p is the pressure and T the temperature. The non-dimensional parameters that govern the flow are the Rayleigh number Ra, the Prandtl number Pr, the non-dimensional gap δ and the tilt angle γ.

The boundary conditions are:

$$u=v=0 \quad \text{at the solid boundaries;}$$

$$\begin{aligned} T=1 \quad &\text{for} \quad 0\leqslant x\leqslant 1, && y=0\\ &\text{and} \quad \delta\leqslant x\leqslant 1-\delta, && y=\delta;\\ T=0 \quad &\text{for} \quad 0\leqslant x\leqslant 1, && y=1\\ &\text{and} \quad \delta\leqslant x\leqslant 1-\delta, && y=1-\delta; \end{aligned}$$

$$\begin{aligned} \frac{\partial T}{\partial x}=0 \quad &\text{for} \quad 0\leqslant y\leqslant 1, && x=0\\ &\qquad \delta\leqslant y\leqslant 1-\delta, && x=\delta\\ &\qquad 0\leqslant y\leqslant 1, && x=1\\ &\text{and} \quad \delta\leqslant y\leqslant 1-\delta, && x=1-\delta. \end{aligned}$$

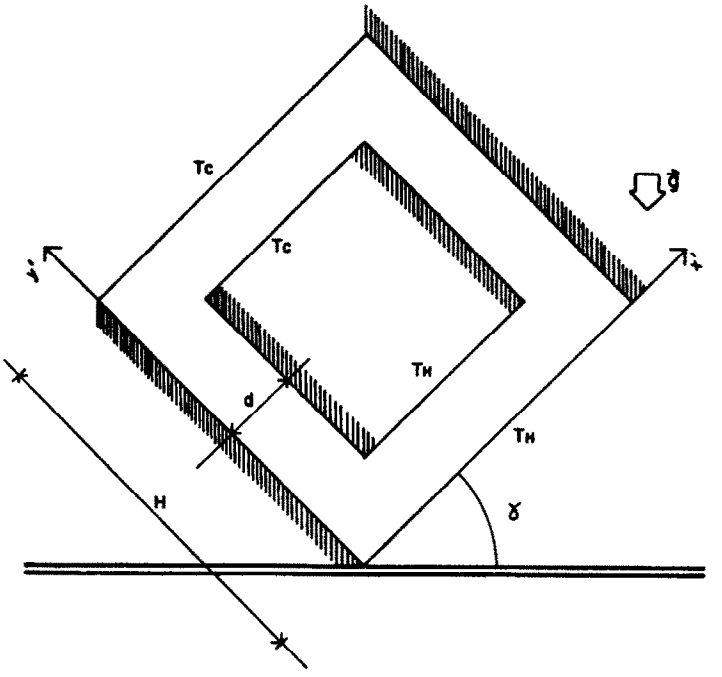

FIG. 1. The two-dimensional square thermosyphon.

For future reference, we shall define the local Nusselt number as

$$Nu(x) = \frac{d}{T'_H - T'_C}\frac{\partial T'}{\partial y'} = \delta\frac{\partial T}{\partial y}$$

which is obviously a function of the position. Due to the geometry of the problem, four Nusselt numbers can be defined, one at each wall at constant temperature.

The numerical solution of the system was obtained using a method similar to the SIMPLE algorithm developed by Patankar and Spalding [12], which is embodied in the PHOENICS code of Spalding [13]. The system of equations is solved using a primitive, dimensional-variables formulation. The non-dimensional formulation adopted here is favored in order to simplify the generalization of results.

A uniform grid with 30×30 control volumes in the x- and y-directions was used to obtain all the results presented in this paper. The central volumes of the square are blocked; a solution is considered to be correct when it has converged and is grid independent. The convergence is attained when the overall sum of the residuals in the mass, momentum and energy equations is less than 0.1% of the total corresponding quantity contained in the integration domain, and the heat balance due to sources and sinks, including the boundaries, is better than 1%. The grid-independent solution is established by comparing the velocity and temperature fields for two converged solutions obtained with different grid spacing. It must be stressed that different grid sizes may require a different number of sweeps to converge. This is also true for different tilt angles. A grid-independence study was carried out and the results obtained with an equally-spaced 60×60 volume grid were found to be in qualitative agreement with those presented here; small quantitative differences (never larger than 15%) were found. Due to the much longer time required to run the program, it was decided to use the 30×30 grid. The number of sweeps and the CPU time required to find the solution in an HP-9000 series 500 computer with a UNIX 5.05 operative system are given in Table 1.

3. RESULTS

3.1. *General features*

Results were obtained for tilt angles ranging from $-180°$ to $180°$ and from $Ra = 10^3$ to 8×10^3. The Prandtl number was fixed at $Pr = 5.5$ and the gap width δ was equal to 0.2 in all cases.

The stream function and temperature fields for $Ra = 4 \times 10^3$ and $\gamma = 0°$, $90°$ and $180°$ are shown in

Table 1. Numerical data for solutions using an HP-9000 series 500 computer

Tilt angle γ	Number of sweeps	Processing time (s)
0°	200	1964
90°	60	632
180°	420	4696

Figs. 2–4. For $\gamma = 0°$ (Fig. 2(a)) the fluid moves around the loop in a counter-clockwise direction except for two small recirculating regions near the lower-left and upper-right corners where the fluid moves in a clockwise direction. The global cell modifies dramatically the temperature field inside the loop from that obtained in the pure conductive case; the isotherms are swept away by the motion of the fluid (Fig. 2(b)). The fluid inside the vertical, thermally insulated legs is almost isothermal while strong temperature gradients are present in the sections corresponding to the constant wall temperature legs; the steepest gradient is located at the horizontal, lower-left and upper-right corners where the fluid enters the hot- and cold-wall temperature regions respectively. The origin of the recirculation regions is in fact due to geometrical

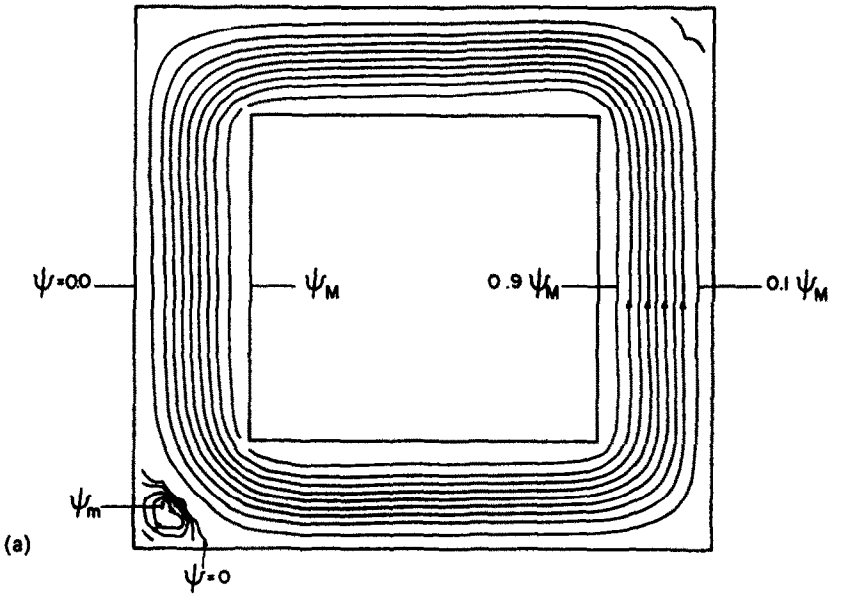

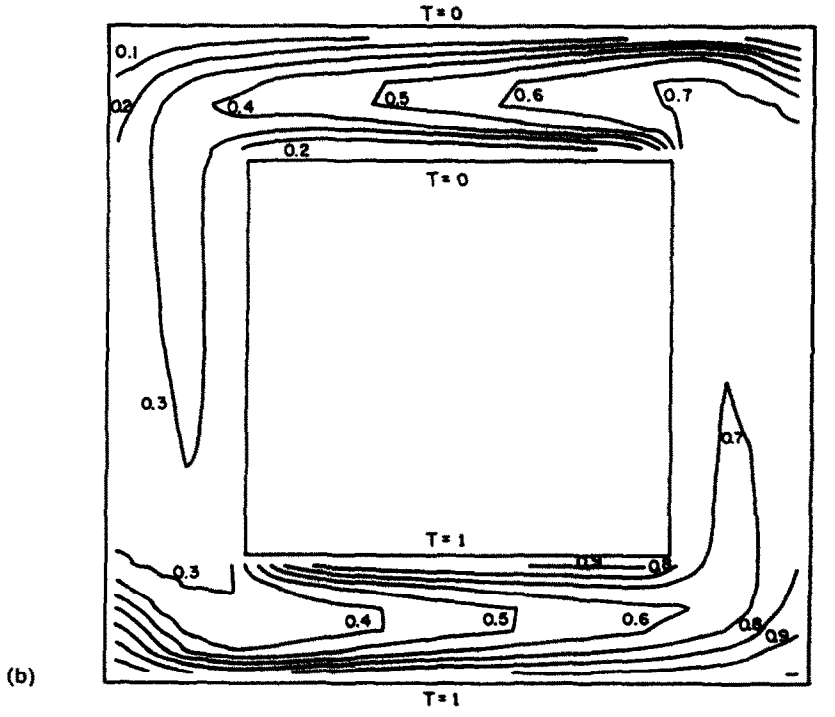

FIG. 2. (a) Stream function and (b) temperature fields for $Ra = 4 \times 10^3$ and $\gamma = 0°$; $\Psi_m = -0.19$, $\Psi_M = 6.5$. (c) Pressure field and (d) center-line pressure for $Ra = 4 \times 10^5$ and $\delta = 0°$.

(c)

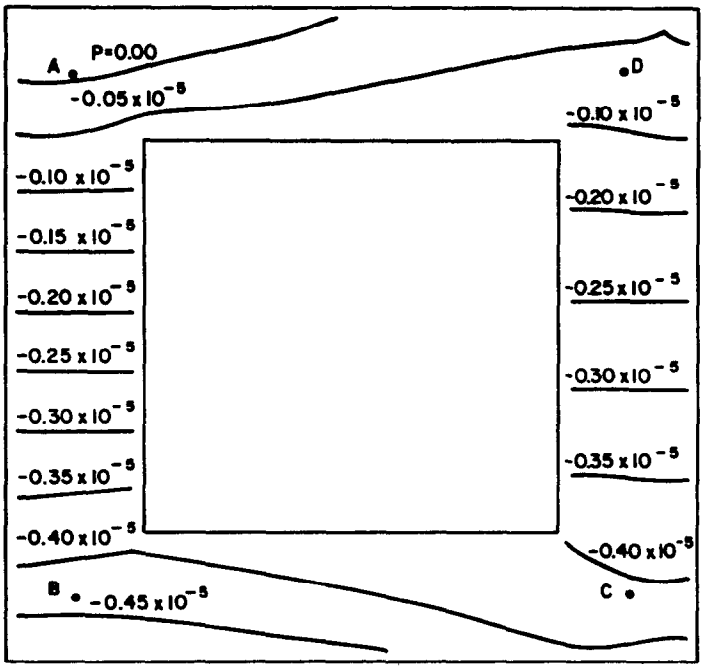

(d)

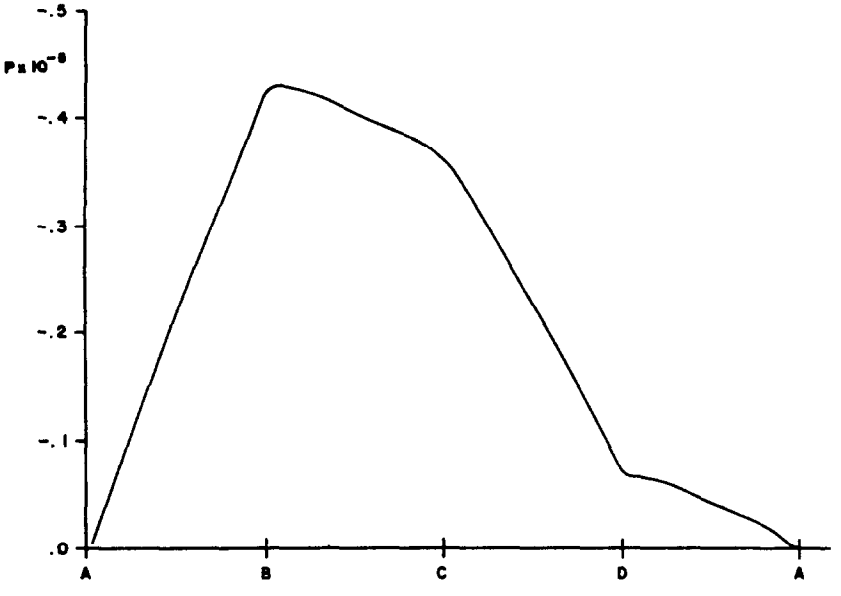

FIG. 2—*continued.*

effects; the fluid tends to remain almost stagnant near the corners, and it is there that horizontal temperature gradients are generated due to the global motion. Therefore, adequate conditions are given locally to form convective cells. Notice, however, that in the lower-right and upper-left corners the temperature gradients tend to generate cells of fluid rotating in the counter-clockwise direction; this motion is opposed by the global cell motion which is far stronger. In contrast, the global cell motion tends to reinforce the local motion in the lower-left and upper-right corners. The largest local recirculation region is formed in the lower-left corner where the generated horizontal temperature gradients are greatest. The pressure field and the pressure along the center-line of the duct is shown in Figs. 2(c) and (d), respectively. The reference pressure $p = 0$ is taken at the uppermost left-hand side corner, with the overall pressure gradient generating a counter-clockwise motion. The flow in the $\gamma = 90°$ case, shown in Fig. 3(a), is similar to the one just described, since a single global cell of fluid circulating in the counter-clockwise direction is formed. The iso-

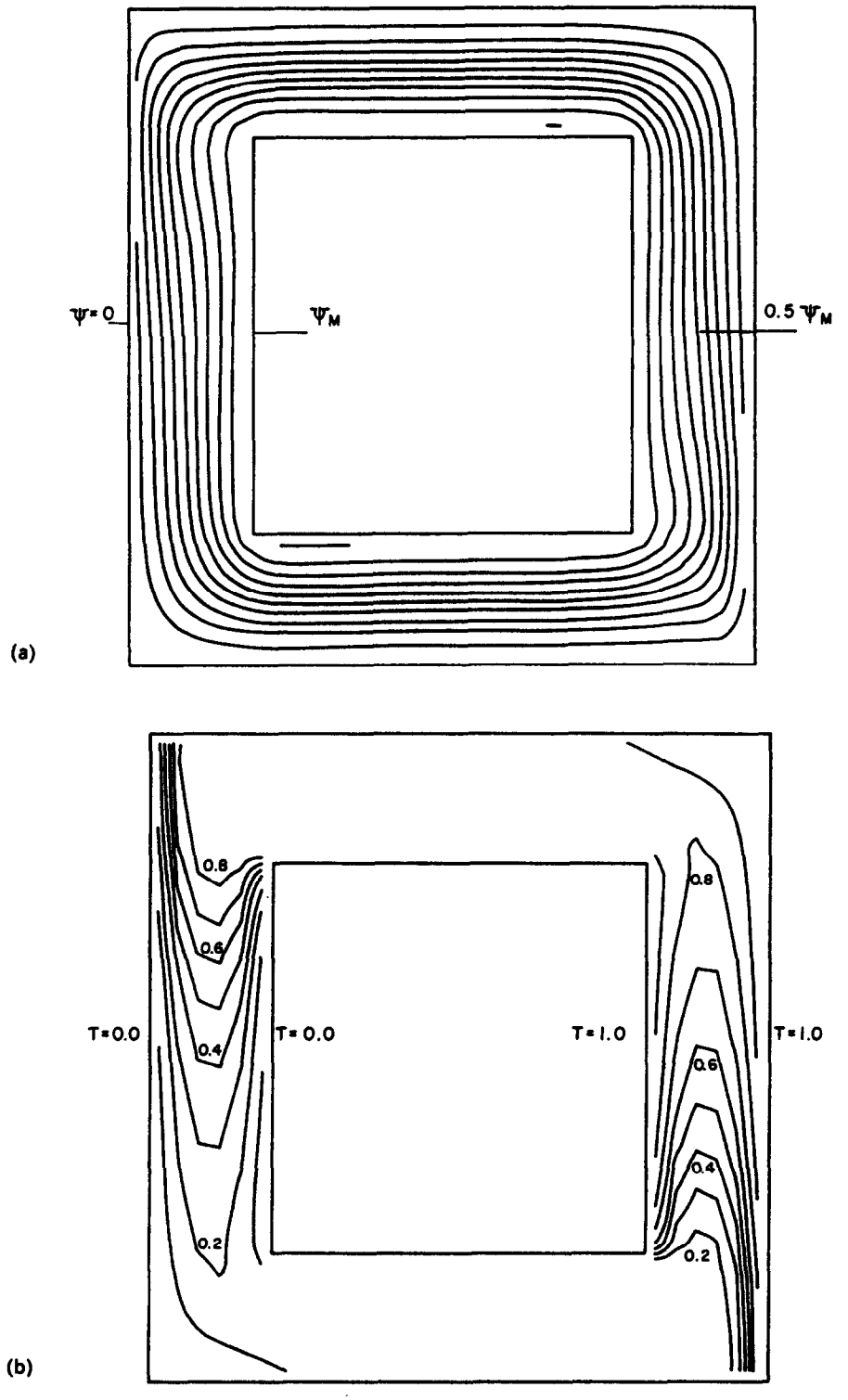

FIG. 3. (a) Stream function and (b) temperature fields for $Ra = 4 \times 10^6$ and $\gamma = 90°$; $\Psi_m = 0.0$, $\Psi_M = 3.5$.

therms also display similar features, but in the present case large temperature gradients are formed in the vertical, constant wall temperature legs, while the flow in the horizontal legs is nearly isothermal. This temperature field configuration does not favor the generation of local cells since only small horizontal temperature gradients are formed at the lower-left and upper-right corners. The stream function and temperature fields for $\gamma = 180°$ are shown in Fig. 4. The fluid remains practically motionless in the straight

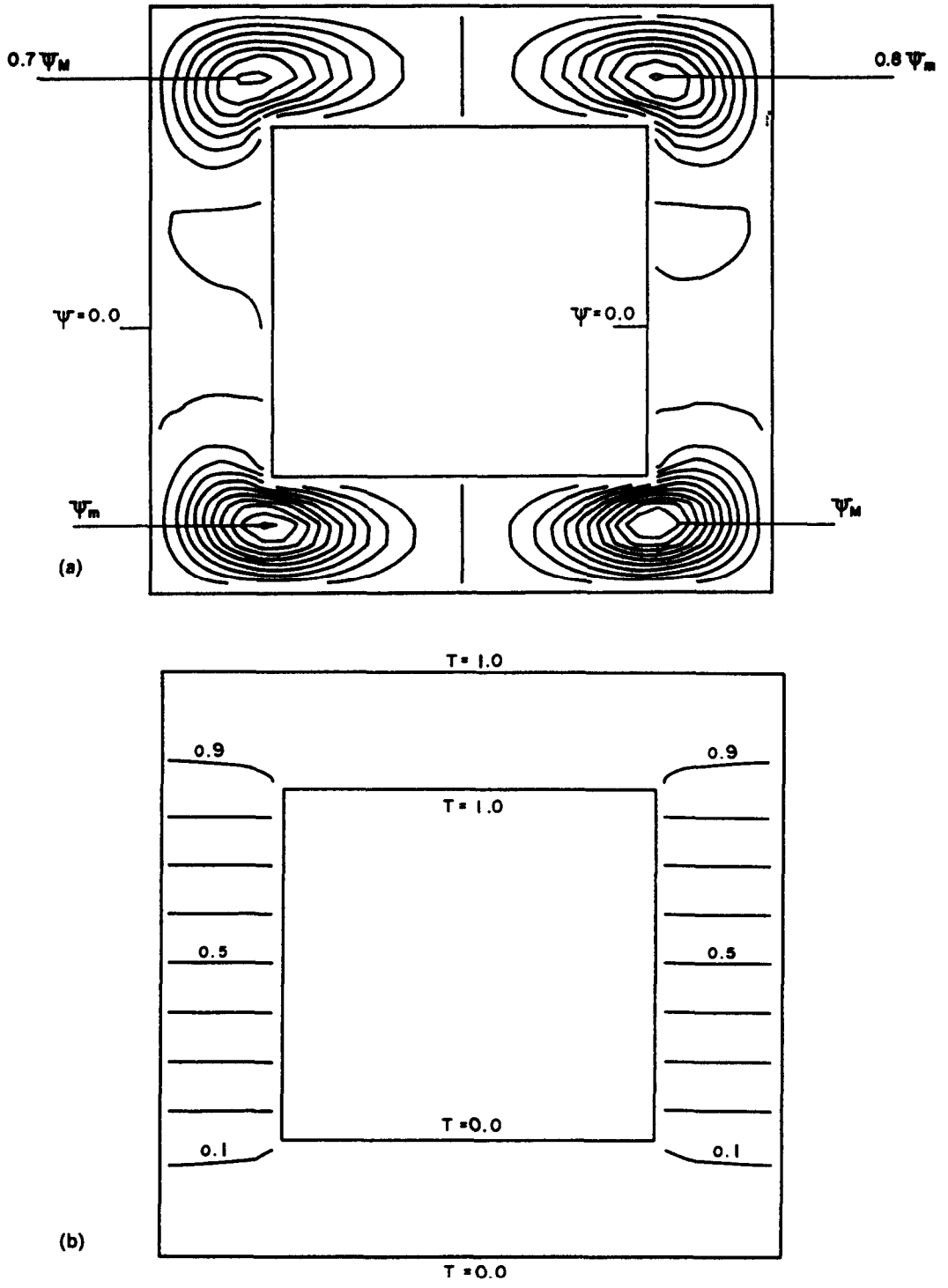

FIG. 4. (a) Stream function and (b) temperature fields for $Ra = 4 \times 10^3$ and $\gamma = 180°$; $\Psi_m = -0.14$, $\Psi_M = 0.14$.

parts of the loop, but four local convection cells are formed near the corners. The temperature field is very similar to that of pure conduction, convection playing only a minor role except near the inner corners where the flow attains its maximum velocity. Two cells circulate clockwise while the other two circulate in the opposite direction. In the upper horizontal leg, the fluid ascends near the center where the hottest region of the loop is located and descends near the corners. This pattern is reversed in the lower horizontal leg where the coldest region is located near its center. Heat is transferred from the hot boundaries of the

loop to the cold ones purely by conduction. The presence of the cells can easily be explained since, locally, the external heating is not uniform and therefore horizontal temperature gradients are present which trigger the motion. The local motions found in this case are similar to the recirculating flows observed in the $\gamma = 0°$ case in the sense that they are driven by local non-homogeneous heating. In the present case, however, the global motion of the fluid does not influence the formation of recirculating patterns as these appear when the global circulation of the fluid is absent.

The transition from a single global cell to multiple local cells as the tilt angle goes from 90° to 180° for $Ra = 4 \times 10^3$ is shown in Fig. 5 (the stream flow lines for $\gamma = 90°$ and 180° are shown in Figs. 3(a) and 4(a), respectively). The pattern changes are smooth. At $\gamma = 120°$, the stagnant regions at the upper- and lowermost corners grow and the streamlines in the regions close to the horizontal corners display curvatures larger than required to turn around the corner. Recall that the fluid enters the constant wall temperature legs at these regions and large temperature gradients are generated therein. When the tilt angle is 150° (Fig. 5(b)), two small recirculating regions develop in these

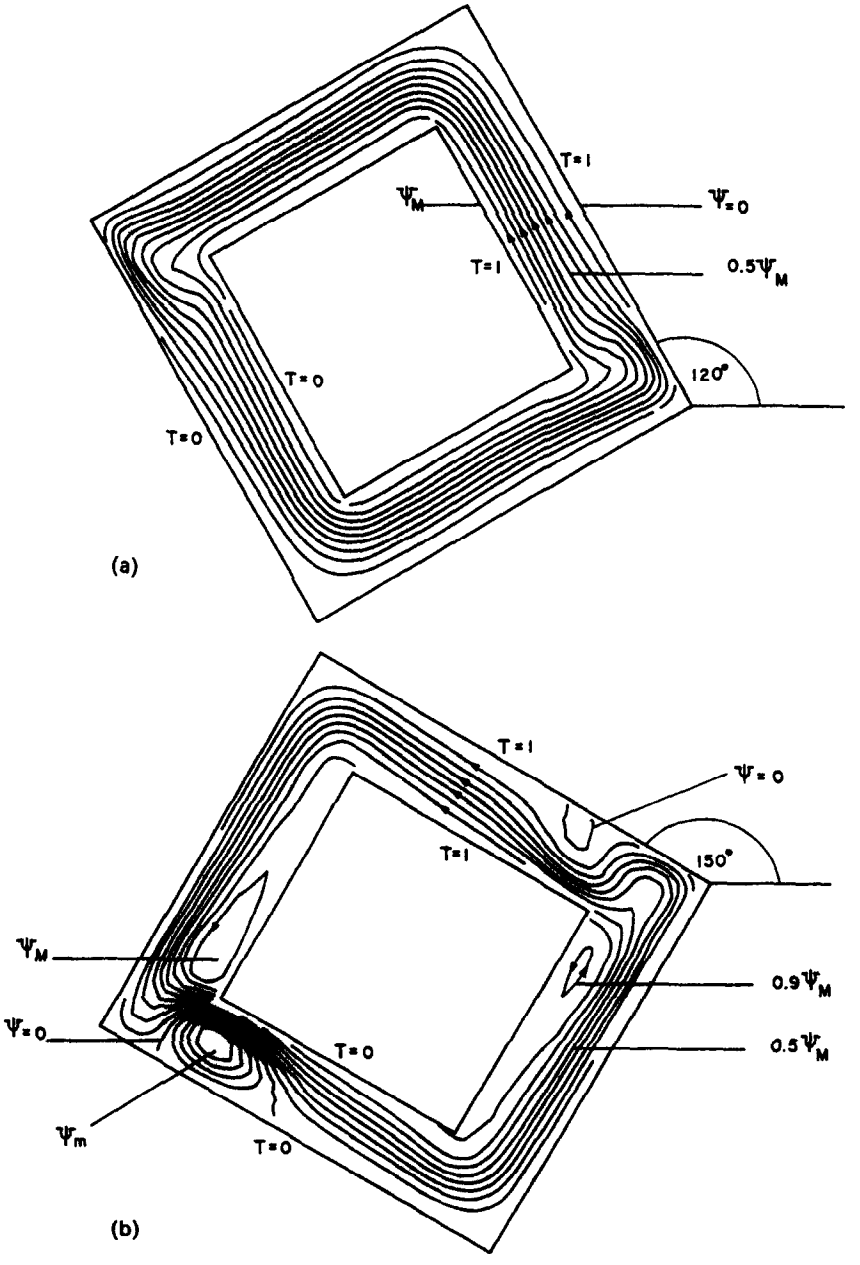

FIG. 5. Stream function fields for $Ra = 4 \times 10^3$. (a) $\gamma = 120°$; $\Psi_m = 0.0$, $\Psi_M = 1.3$. (b) $\gamma = 150°$; $\Psi_m = -0.1$, $\Psi_M = 0.2$. (c) $\gamma = 170°$; $\Psi_m = -0.15$, $\Psi_M = 0.15$. (d) $\gamma = 175°$; $\Psi_m = -0.14$, $\Psi_M = 0.14$.

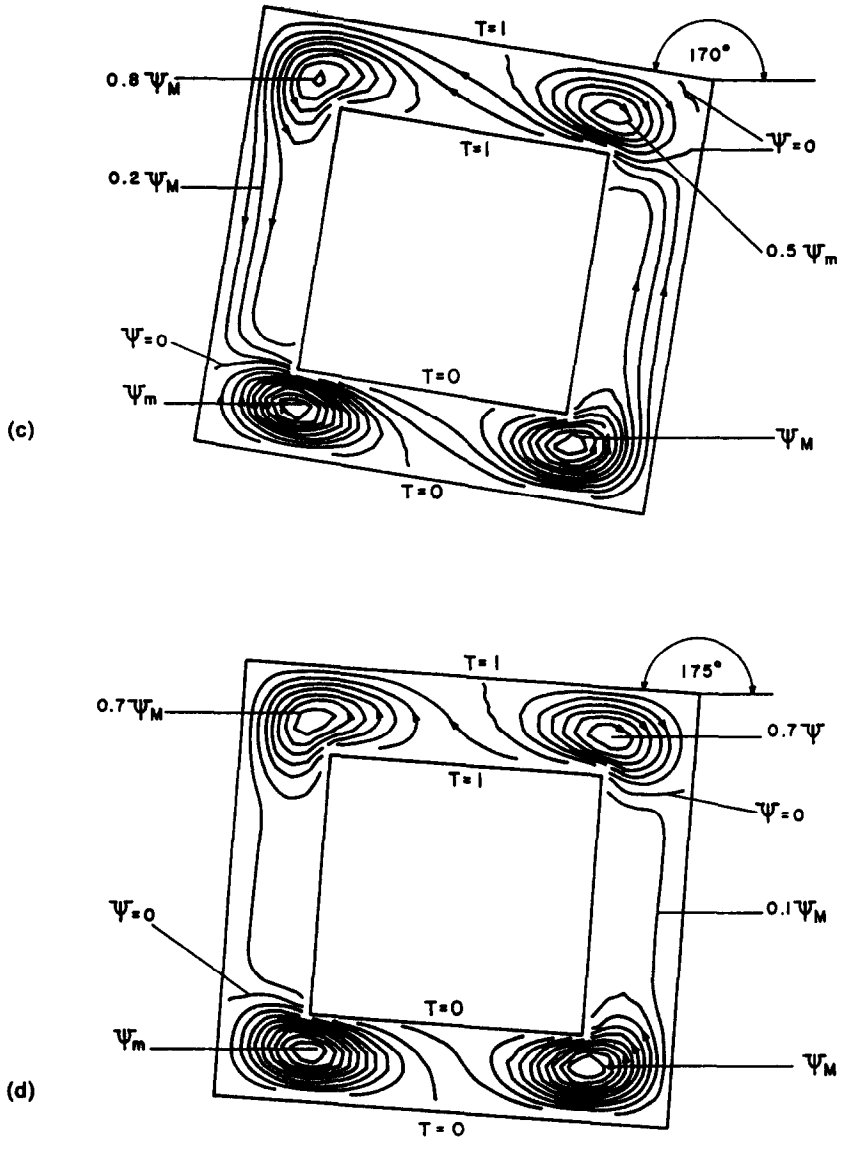

FIG. 5—*continued.*

corners. At $\gamma = 170°$ (Fig. 5(c)) recirculating regions are formed at the four corners; those at the upper- and lowermost corners circulate in the same direction as the global cell while the other two circulate in the opposite direction. For $\gamma = 175°$ (Fig. 5(d)) the four cells are nearly symmetric and the global cell has practically disappeared. The local cells grow stronger and larger and the global cell weakens as the tilt angle approaches $\gamma = 180°$.

3.2. *Multiple solutions*

The flow inside the loop can be characterized by specifying the value of the stream function Ψ at the inner wall and assuming a value of $\Psi = 0$ at the outer wall. For fixed δ, Ψ at the inner wall is proportional to the mean global flow. Also, positive (negative) values of Ψ indicate counter-clockwise (clockwise) global rotation. Using a similar method as discussed by Moya *et al.* [14] the map of possible solutions as functions of the tilt angle, shown in Fig. 6, was found, where velocity versus tilt angle plots resemble S-shaped curves and are cross-sections of a cusp catastrophe. Results were obtained for $Ra = 10^3$, 4×10^3 and 8×10^3. Two solutions are present in the region near zero tilt angle. Following other studies (see for instance refs. [10, 14]), we shall call 'natural' flows those located in the first and third quadrants, since the fluid moves upwards in the hot temperature leg and downwards in the cold temperature one; flows in the second and fourth quadrants are called 'anti-natural'.

The critical angles where the system flowing in one direction switches to the other are $-41°$, $-38°$ and $-29°$ for $Ra = 10^3$, 4×10^3 and 8×10^3, respectively. This result is in qualitative agreement with experimental observations in a square loop with circular

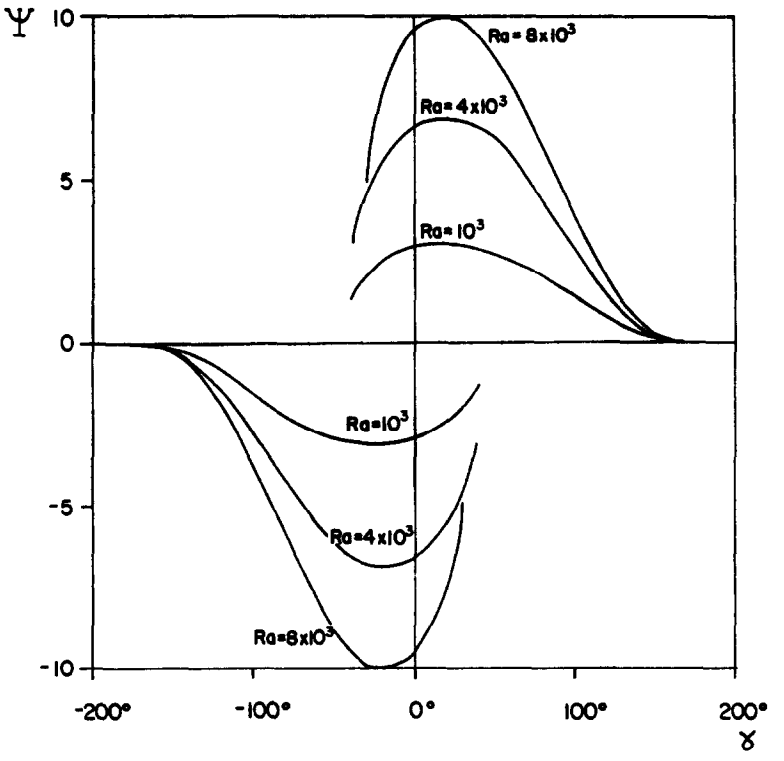

FIG. 6. Stream function at the inner wall as a function of the tilt angle.

cross-section [10] insofar that the larger the heat transferred by the system, the smaller the critical tilt angle. The flow patterns at near-critical tilt angles are shown in Figs. 7(a) and (b) for $Ra = 4 \times 10^3$. Local recirculating regions appear close to the corners aligned with the horizontal axis when the flow is anti-natural; the flow in these regions becomes stronger as the tilt angle approaches its critical value. The circulation in the local cells is 'natural' in the sense that fluid moves upwards near the hot wall and downwards near the cold wall. These regions contribute to minimize the buoyant effect driving the anti-natural motion since the flow of the left-hand corner recirculation cell conveys heat from the hot wall to the cold fluid before it actually enters into the hot leg. Heat is removed from the fluid in the global cell at the right-hand corner before it enters into the cold leg. The formation of local cells also has the effect of reducing the area available for the global circulation. The fact that the critical tilt angle is smaller for larger Rayleigh numbers can be qualitatively explained in terms of the presence of local recirculations, as they are stronger for larger Rayleigh numbers. This effect can be observed by comparing Figs. 7(a) and 8, showing the streamlines for anti-natural flow near the critical tilt angle for $R = 4 \times 10^3$ and 8×10^3, respectively.

The change in the direction of circulation has been interpreted using one-dimensional theories in terms of the catastrophe theory [11]. The set of steady-state values of the velocity can form a cusp catastrophe in the parameter space and not two but three velocities are found in the vicinity of the zero-tilt region. It is clear that only two out of the three velocities are stable and therefore the third one cannot be experimentally or numerically found. In the present two-dimensional model it is difficult to demonstrate that steady-state velocities form a two-dimensional manifold displaying a cusp catastrophe in the parameter space; however, it is clear that the qualitative features are similar to those found in one-dimensional systems and therefore a similar kind of model will be appropriate to describe the phenomenon.

3.3. *Heat transfer*

The behavior of the loop as a 'heat-pump' can be assessed from Figs. 9 and 10 where the local Nusselt number at the outer hot wall is plotted as a function of position for the three cases presented in Figs. 2–4. Local Nusselt number profiles for the cases where a global cell is present display a maximum near the upstream corner of the wall where the cold fluid meets the hot wall. This maximum is never further away from the upstream corner than a distance equal to the gap; the minimum of the local Nusselt number is always located in the downstream corner where the fluid has almost reached thermal equilibrium with the wall (see Fig. 9). The local cells that appear in the $\gamma = 180°$ case reduce the local Nusselt number at the corners, since they move hot fluid from the internal hot wall towards the external one. The total heat

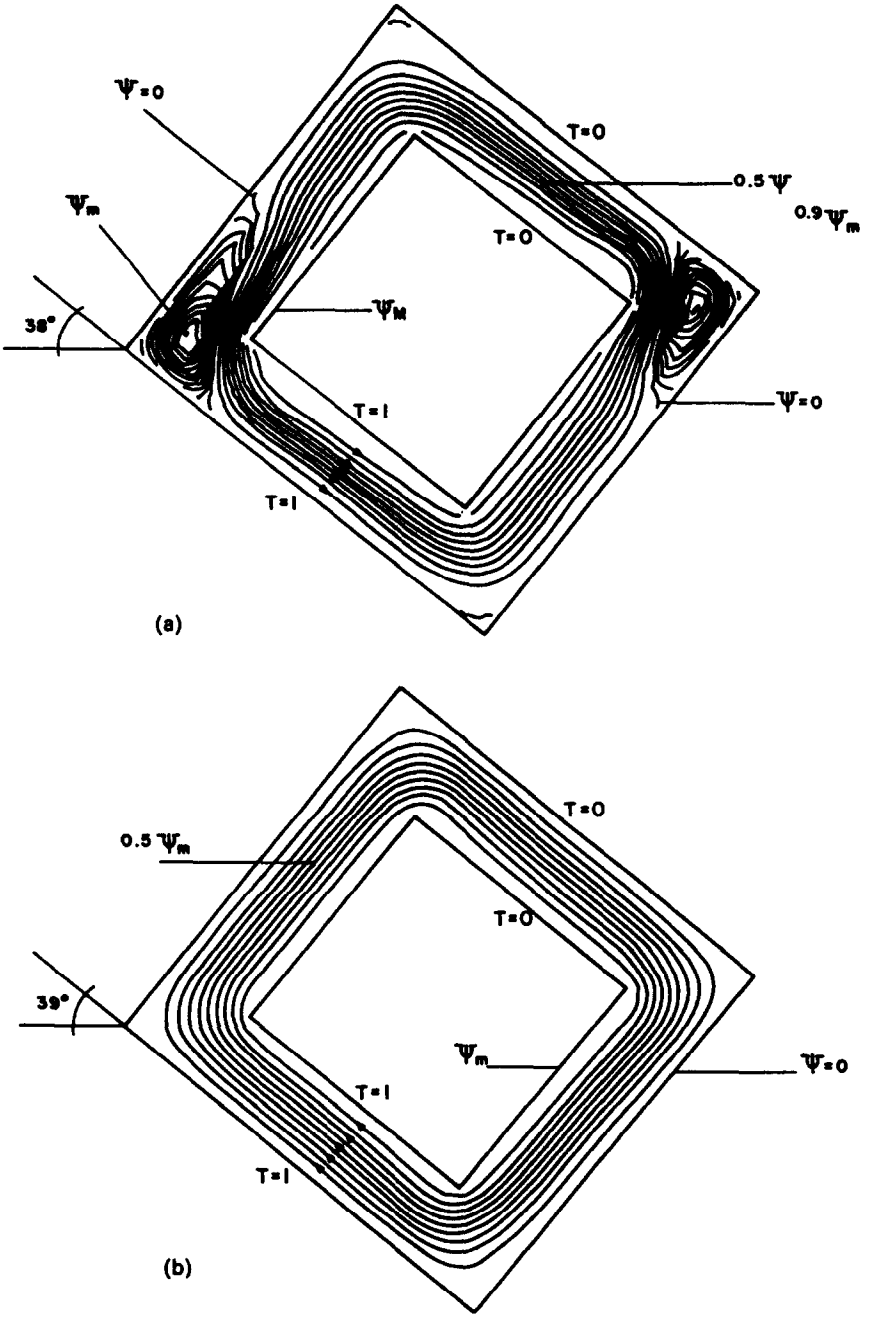

FIG. 7. Stream function for $Ra = 4 \times 10^3$ near the critical angle. (a) $\gamma = -38°$; anti-natural flow. (b) $\gamma = -39°$; natural flow.

transferred by the system is hardly any different than that obtained with pure conduction, as it can be seen from Fig. 10. The Nusselt numbers for $\gamma = 180°$ are more than one order of magnitude smaller than those for $\gamma = 0°$ or 90°, showing the very important role of the global convective cell on the total heat transferred.

4. DISCUSSION AND CONCLUSIONS

Some features of the two-dimensional flow of a natural convective loop have been studied. Flows with either a single global cell or with a number of local cells have been found by varying the tilt angles. The recirculating regions appearing in the $\gamma = 0°$ case originate from effects similar to those described by Lavine *et al.* [8] for small tilt angles. In addition, the absence of recirculating regions for $\gamma = 90°$ is common to the square and toroidal loops. Unfortunately, there are no results for a toroidal loop with $\gamma = 180°$ but it is likely that local cells would form, at least in 'fat' loops. It can be reasonably expected that four cells would form, each of them extending to one-quarter of the loop.

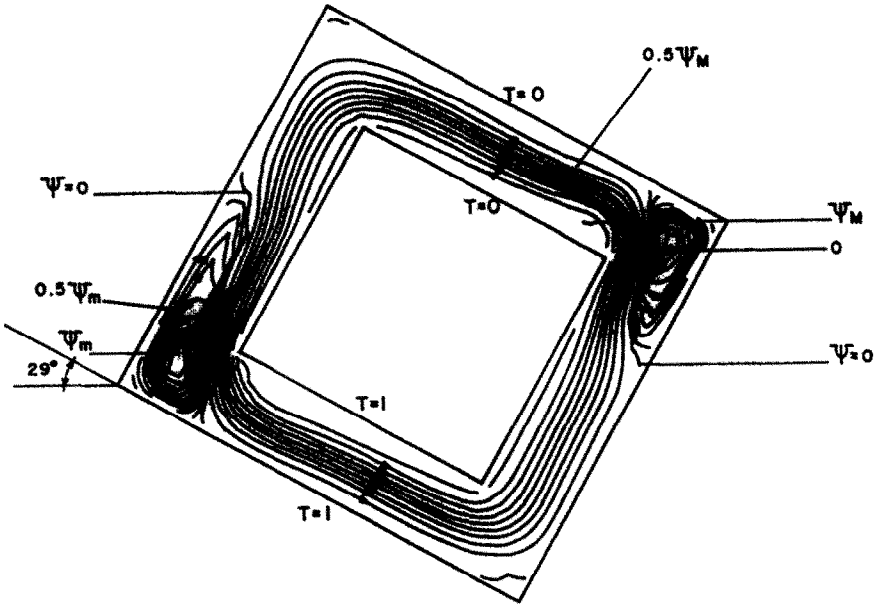

FIG. 8. Stream lines for $Ra = 8 \times 10^3$ near the critical angle; $\gamma = -29°$, anti-natural flow. $\Psi_m = -1.6$, $\Psi_M = 5.1$.

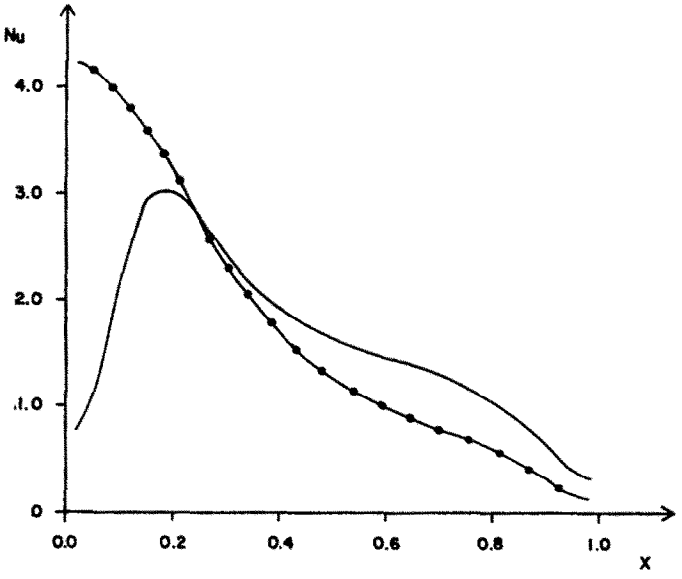

FIG. 9. Local Nusselt number at the external hot wall as a function of position for $Ra = 4 \times 10^3$ and $\gamma = 0°$ (——) and $\gamma = 90°$ (●—●).

The existence of multiple solutions in a two-dimensional loop has been demonstrated using a model where no empirical information is required. The steady-state mass flow rate seems to form a cusp catastrophe in the tilt angle–Rayleigh number space in a similar way to that described by one-dimensional theory. In the case of the two-dimensional model, the fact that the 'anti-natural' solution changes into the 'natural' solution seems to be due to the presence of the local recirculations; however, the qualitative form of the Ra–γ map is remarkably similar to its one-dimensional counterpart, indicating that the mechanism controlling the stability is not contained only in the two-dimensional, local recirculation effects.

Recirculating flows were found under three different conditions: (a) horizontal heating on the top, (b) horizontal heating on the bottom, and (c) near the critical tilt angle. Their presence is due to local heating conditions. Two different convective pattern changes were identified as functions of the tilt angle. As the system is tilted from 90° to 180°, the pattern evolves smoothly from the one global cell to four local con-

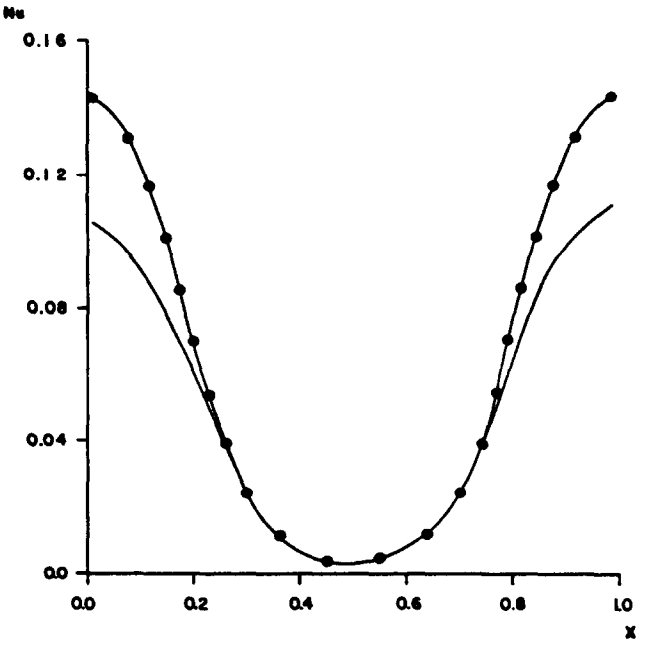

FIG. 10. (——) Local Nusselt number at the external hot wall as a function of position for $Ra = 4 \times 10^5$ and $\gamma = 180°$. (●—●) Local Nusselt number for pure conduction.

vective cells. However, when the system is tilted from anti-natural to natural flow past the critical angle, the pattern changes abruptly from one main global cell with recirculation regions into a single cell rotating in the opposite direction. It is striking that the large differences in the flow patterns shown in Figs. 7(a) and (b) are produced by a change of only one degree of inclination.

The natural extension of the present study is the analysis of the time evolution of the flow. According to one-dimensional theory, the flow may evolve to acquire a constant steady-state velocity or aperiodic oscillations. This analysis is presently in progress.

REFERENCES

1. A. Mertol and R. Greif, A review of natural circulation loops. In *Natural Convection: Fundamentals and Applications* (Edited by W. Aung, S. Kakaç and R. Viskanta), pp. 1033–1071. Hemisphere, New York (1985).
2. H. F. Creveling, J. F. De Paz, J. Y. Baladi and R. J. Schoenhals, Stability characteristics of a single-phase free convection loop, *J. Fluid Mech.* **67**, 65–84 (1975).
3. W. V. R. Malkus, Non-periodic convection at high and low Prandtl numbers, *Mem. Soc. R. Sci. Liege 6 Ser.* **IV**, 125–128 (1972).
4. M. Sen, E. Ramos and C. Treviño, The toroidal thermosyphon with known heat flux, *Int. J. Heat Mass Transfer* **28**, 219–233 (1985).
5. J. E. Hart, A new analysis of a closed loop thermosyphon, *Int. J. Heat Mass Transfer* **27**, 125–136 (1984).
6. A. Mertol, R. Greif and Y. Zvirin, Two-dimensional study of heat transfer and fluid flow in a natural convection loop, *J. Heat Transfer* **104**, 508–514 (1982).
7. A. Mertol, R. Greif and Y. Zvirin, Two-dimensional analysis of transient flow and heat transfer in a natural circulation loop, *Wärme- und Stoffübertr.* **18**, 89–98 (1984).
8. A. S. Lavine, R. Greif and J. A. C. Humphrey, A three-dimensional analysis of natural convection in a toroidal loop—the effect of the tilt angle, ASME Paper No. 85/WA-7 (1985).
9. P. S. Damerell and R. J. Schoenhals, Flow in a toroidal thermosyphon with angular displacement of heated and cooled sections, *J. Heat Transfer* **101**, 672–676 (1979).
10. R. Acosta, M. Sen and E. Ramos, Single-phase natural circulation in a tilted square loop, *Wärme- und Stoffübertr.* **21**, 269–275 (1987).
11. M. Gordon, E. Ramos and M. Sen, A one-dimensional model for a thermosyphon with known wall temperature, *Int. J. Heat Fluid Flow* **8**, 177–181 (1987).
12. S. V. Patankar and D. B. Spalding, A calculation procedure for heat, mass and momentum transfer in three-dimensional parabolic flows, *Int. J. Heat Mass Transfer* **15**, 1787 (1972).
13. D. B. Spalding, A general purpose computer program for multi-dimensional one- and two-phase flow. In *Math. Comp. Sim.*, Vol. XXIII, p. 267. North-Holland, Amsterdam (1981).
14. S. L. Moya, E. Ramos and M. Sen, Numerical study of natural convection in an inclined porous material, *Int. J. Heat Mass Transfer* **30**, 741–756 (1987).

CONVECTION NATURELLE DANS UNE BOUCLE CARREE BIDIMENSIONNELLE

Résumé—On étudie la convection naturelle permanente dans une boucle bidimensionnelle carrée. Les montants opposés de la boucle sont maintenus à des températures uniformes différentes ce qui induit un mouvement du fluide du à la pesanteur; l'effet de la viscosité est de s'opposer au mouvement et on atteint un régime permanent. La géométrie de la boucle est fixée mais on considère plusieurs différences de température. On analyse aussi l'effet de l'angle d'inclinaison sur les configurations d'écoulement. Des mouvements locaux de recirculation apparaissent lorsque les parois supérieures sont à des températures plus élevées que les parois inférieures. Par contre, une cellule globale unique apparait quand la boucle est inclinée. Des solutions doubles ont été trouvées pour des angles d'inclinaison proche de zéro (température élevée aux parois inférieures); la taille de l'intervalle d'angle d'inclinaison, quand les solutions doubles existent, a été déterminée en fonction du nombre de Rayleigh. Des modèles monodimensionnels ont donné des solutions permanentes multiples dans des systèmes semblables à celui étudié ici; on démontre, dans cette étude, l'existance des solutions multiples dans un modèle bidimensionnel.

NATÜRLICHE KONVEKTION IN EINER ZWEIDIMENSIONALEN QUADRATISCHEN SCHLEIFENANORDNUNG

Zusammenfassung—In dieser Arbeit wird die stationäre natürliche Konvektionsströmung in einer zweidimensionalen quadratischen Schleifenanordnung untersucht. Gegenüberliegende Teile dieser Schleife werden auf konstanter, aber unterschiedlicher Temperatur gehalten, was in Anwesenheit eines Schwerefeldes eine Fluidbewegung sicherstellt. Die Bewegung wird durch Reibungskräfte begrenzt, wodurch sich eine stationäre Strömung einstellt. Es wird mit konstant gehaltender Geometrie der Schleifenanordnung gearbeitet, die Temperaturdifferenz ist jedoch unterschiedlich. Außerdem wird der Einfluß des Neigungswinkels auf die Strömungsformen untersucht. Wenn die oberen Wände eine höhere Temperatur aufweisen als die unteren, kommt es regelmäßig zu lokalen Rückströmungen. Falls die Schleifenanordnung geneigt ist, tritt eine einzelne globale Zelle in Erscheinung. Es ergeben sich Zweifachlösungen für Neigungswinkel nahe 0 (hohe Temperatur an den unteren Wänden). Der Bereich der Neigungswinkel mit Doppellösungen wurde in Abhängigheit von der Rayleigh-Zahl ermittelt. Eindimensionale Modelle haben bereits früher mehrfache stationäre Lösungen in Systemen ähnlich den hier untersuchten erbracht. In der vorliegenden Arbeit wird die Existenz von Mehrfachlösungen in einem zweidimensionalen Modell gezeigt.

ЕСТЕСТВЕННАЯ КОНВЕКЦИЯ В КАНАЛЕ КВАДРАТНОГО СЕЧЕНИЯ

Аннотация—Излагаются результаты исследования стационарной естественной конвекции в двумерном канале квадратного сечения. На противоположных стенках канала поддерживаются постоянные температуры различной величины. Поэтому под действием силы тяжести жидкость приходит в движение, которое благодаря вязкостным эффектам в конечном счете становится устойчивым. При заданной геометрии сечения канала анализируется влияние разностей температур на противоположных стенках на режим течения. Рассмотрено также влияние угла наклона на картины течения. Если температура верхних стенок больше температуры нижних стенок, характерной особенностью течения являются локальные рециркуляционные потоки. При наличии же наклона контура появляется одиночная глобальная ячейка. При близких к нулю углах наклона (при высокой температуре нижних стенок) обнаружены двойные решения. Определена зависимость диапазона значений угла наклона, для которого существует двойное решение, от числа Рэлея. С использованием одномерных моделей получены кратные стационарные решения для систем, аналогичных изученной в данной работе. Показано наличие кратных решений в двумерной модели.